MICROPERIMETRY

VAN DE VELDE F.J.[1, 2]

ABSTRACT

In SLO microperimetry a multi-channel overlay graphics frame grabber synchronizes the scanning of an infra-red laser with the modulation of a visible laser source. Graphics are created in the laser raster with a fast 25 ns sub-pixel rise-time 80 MHz acousto-optic modulator, Bragg angle optimized for 532 nm, 543.5 nm, 632.8 nm or 660 nm wavelengths over a 40 dB attenuation range. Our software kernel comprises 4 alternative forced choice (4AFC), parameter estimation by sequential testing (PEST) and manual or automated tracking algorithms based on two-dimensional normalized gray-scale correlation. They enable fast and accurate registration of fixation patterns, precise measurements of potential acuities and retinal sensitivity using a range of background illumination levels. Opto-electronic characteristics of physiologic significance are discussed. Clinical examples are given.

KEYWORDS

Scanning laser ophthalmoscope, SLO, microperimetry, age related maculopathy, ARM, low vision, retina, laser, psychophysics

RÉSUMÉ

En micropérimétrie SLO, un dispositif d'acquisition d'images graphiques par recouvrement multicanaux permet de synchroniser le balayage d'un laser infra-rouge avec la modulation d'une source laser visible. Les graphiques sont créés dans la trame du laser avec un modulateur acousto-optique de 80 MHz avec un temps de montée rapide de sous-pixel de 25 ns, avec un angle de Bragg optimisé pour des longueurs d'ondes de 532 nm, 543,5 nm, 632,8 nm ou 660 nm sur un intervalle de variation de l'affaiblissement de 40 dB. Notre noyau logiciel comprend 4 choix forcés alternatifs (4AFC), une estimation des paramètres par test séquentiel (PEST) et des algorithmes de pistage manuels ou automatiques, basés sur une corrélation de l'échelle des gris normalisée à deux dimensions. Cela permet d'obtenir un enregistrement rapide et précis des trames de fixage, ainsi que les mesures précises des acuités potentielles et de la sensibilité rétinienne, avec l'utilisation d'une gamme de niveaux d'illumination du fond. Les caractéristiques opto-électroniques possédant une signification physiologique sont en discussion.

MOTS-CLÉS

Ophtalmoscope à balayage laser, SLO, micropérimétrie, maculopathie liée à l'âge, ARM, basse vision, rétine, laser, psychophysique

.....

[1] *The Schepens Retina Associates Foundation and SERI - Harvard University, Boston, MA*
[2] *Department of Ophthalmology, University of Antwerp, Belgium*

INTRODUCTION

The potential destructiveness of optical maser on the retina caught the attention of a team that included Gordon Gould, a recognized co-inventor of this light source who also coined the word ''laser''.[46,75] Nearly back-to-back in the same journal, potential beneficial ophthalmic applications are mentioned for the first time.[76] Pulsed ruby crystal lasers were soon followed-up by continuous wave krypton, argon and He-Ne gas lasers. At the Schepens, Pomerantzeff was an early pioneer in creating laser equipment for retinal photocoagulation.[34] While adhering to the ''Primum nil nocere'' principle, the Retina Associates sought to improve the long-term outcome of the wet type of age related maculopathy by aggressively treating with a laser subfoveal and (sub)retinal neovascular membranes, yet not destroy or even compromise useful vision. Two of their treatment strategies to accomplish this goal are cited. First, blue light, at 488 nm strongly absorbed by the yellow xanthophyll pigment, was filtered out from the argon laser emission to avoid collateral damage to the inner retina and nerve fiber layer in the perifoveal area.[33,59] This approach also permitted frequent retreatments for recurrences. Second, they relied on a fundus kinetic perimetry technique called photofield mapping to determine the extent of dense and relative scotomas as well as the retinal locus of fixation on the retina. Photofield mapping comprised the projection of a fundus color slide onto a correctly oriented visual field taken with the Autoplot.[2,16,22,44-45] A similar technique used the Octopus automated perimeter.[29] Difficult to correct variations in the projection magnification factor and a lack of fixation monitoring reduced however the usefulness of such indirect fundus perimetry. In the sixties a more direct form of an infra-red fundus camera based televised perimetry had been developed, but as mentioned before in this volume infra-red optical fundus imaging lacked the much needed visualization of anatomical details. Therefore this approach was abandoned.[3,14-15,18-20,30] A modernized, computer controlled version of this type of equipment using LCD projection is now available.[53] The SLO approach as documented below solved both problems of spatial ambiguity and low contrast of anatomical detail in the referenced fundus video images.

METHODS

The graphics engine and the acousto-optic modulator

Shortly after the SLO was developed at the Schepens, stimuli were projected onto the retina by inserting a slide, as simple as a pinholed neutral density filter, in a location within the instrument that is confocal with the retinal plane. X-Y translations of the graphics were under motor control.[56] This configuration is reminiscent of the projecting method of Trantas and other attempts to explore retinal functioning.[21,26,58] Since in the early SLO apparatus a single visible laser source was used for both imaging of the retina and psychophysics, stimuli had to be either much darker or even more intense with regard to the effective bleaching light level of the background.

In a succession of technical improvements, Hughes and Webb first introduced elegant 40 MHz acousto-optic modulation of the scanning laser to create the graphics within the laser raster.[69] For this purpose, the modulator was controlled by a standard video-signal from a 4 bit NNGS graphics card inside an Apple IIe computer.[64] Selected analog recorded video frames from the SLO, showing the fundus and decremental stimuli, were then corrected for fixation shifts off-line using a separate larger Digital Equipment Corporation VAX computer.[57] By 1994, the arrival of a new generation of powerful combined graphics and frame grabbing cards for the Pentium based IBM personal computer has allowed us to use a much wider range of stimuli intensities on the retina with a nearly invisible background, and correct for fixation shifts during testing online. Only from this point onward did it become practical to use a nearly invisible scanning infra-red laser of 790 nm solely for the purpose of imaging and a superimposed scanning visible laser

source under acousto-optic modulator (AOM) control exclusively for the purpose of graphics projection.[63]
In our laboratory and in the examples, we have used the Imaging Technology Corporation RGB Overlay Frame Grabber because of its powerful non-destructive overlay graphics capability with near instantaneous look-up table (LUT) transformations, and the capability of synchronizing with phase locked loop (PLL) circuitry the slight irregular timing signals from the SLO with the graphics signal going to the acousto-optic modulator (Fig. 1). At present, a powerful data line buffer can be coupled to a laptop computer through the high speed USB port in order to achieve the same result.[61-62]
The optical part of an AOM that we now prefer to use, is a crystal that is made to vibrate at a frequency of 80 MHz with the help of an attached piezo-transducer. These standing vibrations set up the equivalent of a diffraction grating within the crystal. A laser beam traversing this crystal at the correct small Bragg angle will be diffracted up to 85 % into a first-order beam (Fig. 2 a).[41] The intensity of the first-order diffracted beam is related to the intensity of modulation of the 80 MHz radio-frequency (RF) steering signal that drives the piezo-transducer. In turn, the modulation of the RF current is accomplished with a varying analog voltage, calibrated between 0 and 1 V. This voltage is derived from one or two output video channels of the 8 bit graphics card. In figure 2 d, the light intensity output of the diffracted beam laser beam is graphically related to the 256 bit levels. The resultant ogival curve is fairly easy to obtain for calibration purposes if the duty cycle of the scanning laser raster is properly taken into account. It resembles part of a square sine function that is characteristic of diffraction efficiency and fits nicely to a polynomial of the 5^{th} degree.[62]
Some performance parameters of the AOM are critical for microperimetry. The RF signal can be attenuated over an analog dynamic range of at least 40 dB, with an additional 30 dB during TTL triggered blanking of the vertical retrace of the visible laser source across the raster. A true zero intensity background is not possible because the RF carrier signal cannot be reduced to zero power and a residual luminous efficiency exists at 790 nm. Because an 80 MHz version AOM is used, we can reduce the beam diameter within the AOM with a telescopic arrangement from 1 mm to 200 μm. The characteristic rise-time of the AOM - i.e. the time that is needed for the ultra-sound vibrations to traverse such a 200 micrometer beam - will then be about 25 ns. This is much shorter than the duration of a typical pixel length of 85 ns, as it should be. The time that is needed for the vibration changes to reach the beam is called the AOM delay. It is in the order of 50 microseconds and has to be taken into account when projecting a stimulus onto the retina (Fig. 2 b). This delay is stable and corresponds to a simple translation of the visual field relative to the image. Unlike with fundus cameras coupled to LCD projection, no rotation or magnification is involved. Bragg angles of incidence vary linearly with wavelength (Fig. 2 c). Therefore, if we want to modulate two wavelengths, for example 532 nm and 660 nm and yet use one AOM, a small wedge prism can be introduced for laser beam steering. In addition, to make this work, the deviation angle between the two beams has to be inverted by the telescopic arrangement that also reduces the beam diameter at the same time.

The algorithms and basic psychophysics

For measuring visual acuities associated with a defined retinal location or fixation pattern, we make use of a four alternative forced choice (4AFC) algorithm.[39,55] Details are provided elsewhere.[7] In brief, two correct responses to a letter E orientation leads to a smaller stimulus presentation, each mistake will cause a next larger size E to be projected (Fig. 3). Besides revealing the true location of stimulation on the retina, the psychophysical advantages of such a technique are a reduced bias from examiner and subject alike, and the accuracy, swiftness, and optimal resolution of testing.
Of note is that the SLO has a typical angular resolution of 1.5 minarc per pixel in a 20 degree diagonal field of view raster mode and about 3 minarc per pixel in the low resolution 40 degree

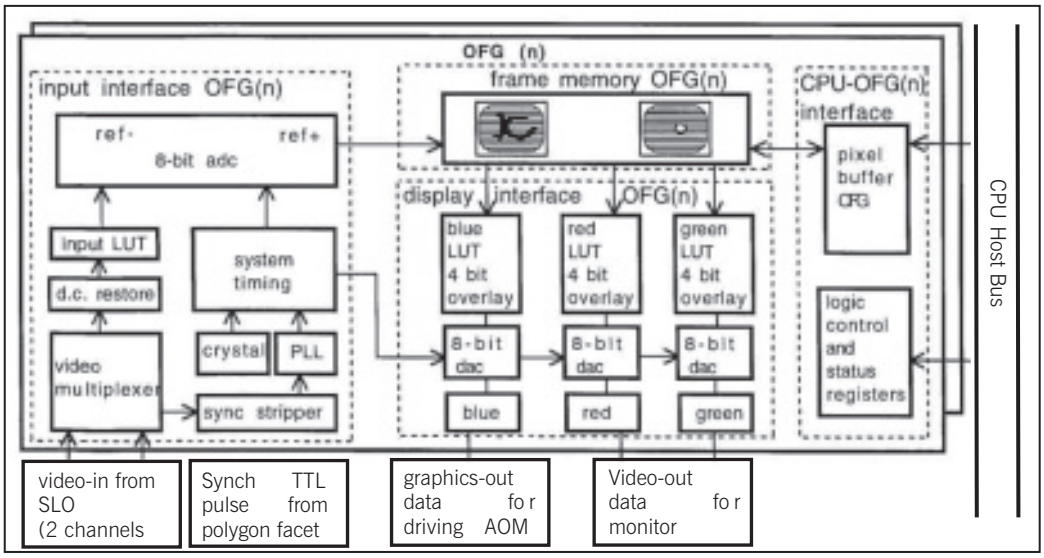

Fig. 1. The Overlay Frame Grabber card design with essential components:(a) the adc converter, (b) polygon sync generator and PLL circuitry, (c) LUT based non-destructive graphics overlay, (d) pixel buffer and dac converter

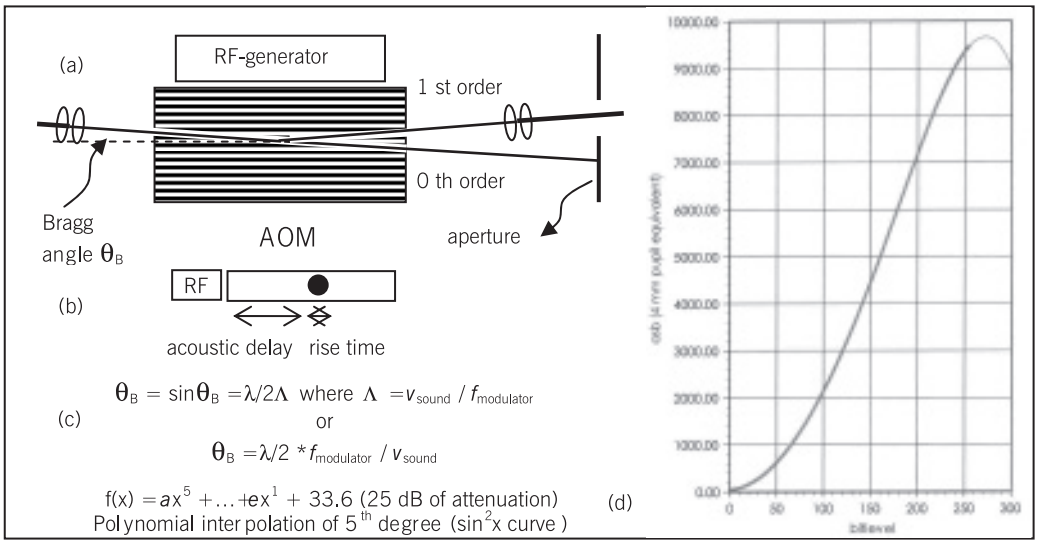

Fig. 2. (a) AOM crystal with acoustic standing wave, Bragg angle, o th and 1st order diffracted beams, (b) sound wave causes acoustic delay and rise time phenomenon, (c) the Bragg angle is a function of wavelength, acoustic sound velocity and driver frequency, a prism may be required for combining wavelengths, (d) calibration curve relating input voltage (bitlevel) to relative 1 st order beam light intensity, interpolation

raster mode. These parameters are ideal to measure low vision acuities with better resolution and sensitivity than conventional charts in the 20/30 to 20/400 range. The high resolution mode is sensitive to defocus because of a limited depth of focus and is also more easily disturbed by scattering. This is not necessarily a drawback but rather an advantage for it enables the estimation of optical quality and spherical refraction for any retinal location within the eye. For example, a 3 diopter hyperopia with ARM may not be measureable with an automated refractometer because of the scar. Also, the low vision television screen is placed at about 33 cm from the eye.

As a result, a 6 diopter lens is required for focusing. We have noticed that several apparent failures in low vision rehabilitation are due to a lack in spherical correction because it is wrongly assumed that the peripheral retina would have no need for such correction.

Using the 4AFC algorithm we have duplicated the peripheral acuity data set obtained by Ludvigh (Fig. 4).[23] Perhaps the most remarkable finding is that even at the isopter of 20 degrees of eccentricity, beyond the optic disc, a useful acuity between 20/150 and 20/200 is possible. The consequences of this are further elaborated upon in the examples.

We prefer to use 100 % decremental contrast letters E with a background that is similar to a bright laptop LCD (Table 1).[9,28] But cone photoreceptors are known to reach their maximum efficiency at 10,000 td,[68] i.e. nearly a half-bleach value of light intensity. In macular pathology we often see low photopic background eccentric fixation patterns switching back to the foveal location for acuity discrimination tasks on a high luminous background. Such patients typically use high intensity lamps at home to keep reading with the fovea. This is a caveat when considering laser treatment for subfoveal lesions. Microperimetry can test for this.

For an accurate determination of retinal sensitivity at a well-defined retinal location we apply a parameter estimation by sequential testing, PEST staircase algorithm to the intensity levels of the stimulus as provided by acousto-optic modulation (Fig. 5). The operational details are described in the references.[4,6-7,54,62] Such adaptive strategy is indicated when uncertainty exists over the most appropriate psychophysical scaling - and this is still the case with microperimetry. Microperimetry has the unique capability to threshold a well-defined location under precise conditions of stimulation, in particular using a minimal background intensity. This background has not been used routinely in the clinic because of difficulties in implementation. The examiner and subject are sitting in a completely darkened environment and the immunity against light level fluctuations caused by a variable light output or changes in pupil diameter is lacking. Using conventional photopic backgrounds, when the Weber-Fechner fraction DI/I is supposed to be near constant, such fluctuations are effectively canceled if the stimulus and background light are derived from the same source.[2,42,44] This does not happen when measuring absolute thresholds. Why would we like to work with a minimal near zero background in the first place? At higher background levels intra-retinal automatic gain controls might mask subtle changes in functioning of the retinal pigment epithelium-photoreceptor complex. If enough quanta are delivered to the retina at higher background levels, any existing deficiency could then be neutralized by means of an adaptive feedback, in a Weber-Fechnerian manner.[68,51]

It is important to be aware of the implications of the Maxwellian type of projection used with the SLO.[70] The entrance location of the illuminating laser beam can be adjusted to avoid media changes, and the amount of stimulus light reaching the retina will vary accordingly. A Stiles-Crawford effect [48-49] may influence thresholds as well. On the fortunate side, the Maxwellian view guarantees a constant flux of light into the eye, regardless of pupil diameter. Also, in a worst case situation, a 3 to 6 dB variability because of the above mentioned factors would likely be overshadowed by an anticipated normal spread of results obtained with untrained subjects in a clinical setting. A new form of perimetry suggested by us might use the Maxwellian view entrance location as a variable while repetitively thresholding at a single retinal location, the fovea.[61] The resultant map can show threshold dependence on media changes, a potential Stiles-Crawford effect and retinal functioning. It could serve as a predictive test for ARM.[5]

Microperimetry uses distinct laser wavelengths. This is an advantage. Beyond 630 nm, the cone system can be selectively studied, at 532 nm or 543 nm it would be the cone-rod or rod system, mostly depending on level of pre-adaptation and background intensity used.[66-67,73-74]

We would like to remind of the pixelated nature of the stimulus in the SLO, which is quite different from the continuous even spatial and temporal intensity distribution of a stimulus in conventional Ganzfeld bowl perimeters. Pixels are turned on individually, for about 85 ns. The pixel fill factor - i.e. how the laser beam profile based on the FWHM diameter relates to the pixel dimension - may be relevant.[36,69] The raster lines of the background are visibly separated under

photopic background conditions. Their separation is galvanometer adjusted to obtain square sized digital pixels. Awareness of these variables is important for further standardization.
Table 1 compares the background illumination and dynamic stimulus range of several perimeters, and includes suggested values for microperimetry. At 632 nm, 1 μW/cm^2 retinal irradiance is equivalent to about 450 trolands, at 532 nm it is equivalent to about 1,800 td.[71-72]

Tab. 1. *Comparison of dynamic range of different type of perimeters*

Perimeter	Background	Maximum Stimulus
Goldmann	31.5 asb (10 cd/m^2)	1,000 asb
Humphrey	31.5 asb	10,000 asb
Octopus	4 asb (1.27 cd/m^2)	1,000 asb
SLO photopic BG	10 cd/m^2 (100 td)	1000 cd/m^2 (3.6 log td)
SLO minimal BG	Minimum intensity	1000 cd/m^2 (9 μW/cm^2)
SLO acuity, EDTRS	240-400 cd/m^2	Minimum intensity
SLO acuity, High BG	2400-4000 cd/m^2	Minimum intensity

The lower end of the dynamic range of stimuli is limited by the Weber-Fechner plateau and the ability to shield the subject from ambient light. The higher end is limited by the effect of the eye optical media scattering causing stray light perception.[8]
The contrast rich infra-red video images provide many fiduciary landmarks that can be used for correction of fixation shifts during microperimetric testing. Three kinds of eye movements have to be dealt with:[27,36-38] (a) a fine 0.5 minarc constant 60 Hz tremor that is mostly irrelevant when considering its frequency and impact on SLO resolution, (b) a slow drifting at the rate of one minarc per second and (c) fast corrective micro saccadic movements back to the (0, 0) motor reference locus of fixation at irregular intervals. The latter two types of eye movements are magnified and more variable when the capability of foveal fixation is lost. Manual tracking of a fiduciary landmark is performed during successive stimulus presentations and aims to correct for the second slow drift variety. Stimulus presentations during saccades are considered invalid. This tracking procedure, outlined in detail elsewhere,[52,57] can also be automated by means of a two-dimensional normalized gray scale correlation digital imaging processing technique.[35,62] Figure 6 illustrates how a reference vessel pattern (a) is retrieved at position (a') within a limited search window (b) in every consecutive video frame.
Microperimetry uses a television type projection system. In general, a higher refresh rate of the scanning laser raster and an interlaced rather than progressive format is helpful. For the purpose of psychophysics a minimum refresh rate of 48 Hz would be required to avoid the sensation of flicker.[74] Innovative laser raster formats dedicated to low vision applications and microperimetry are being developed in our laboratory.

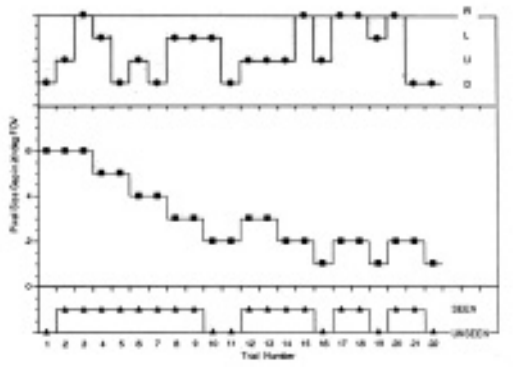

Fig. 3. "4 AFC" algorithm

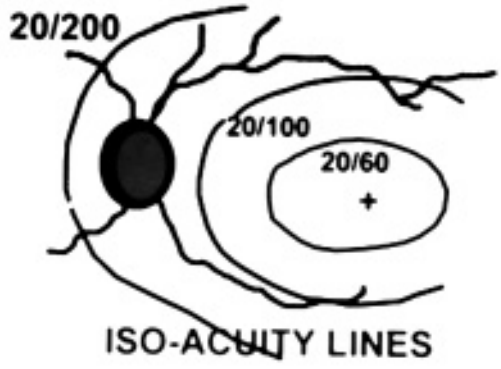

Fig. 4. Potential acuity isopters

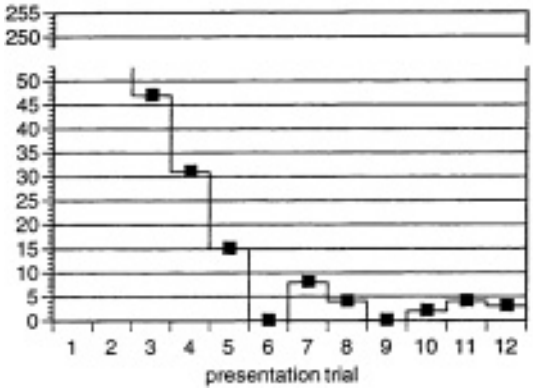

Fig. 5. ''Pest'' algorithm

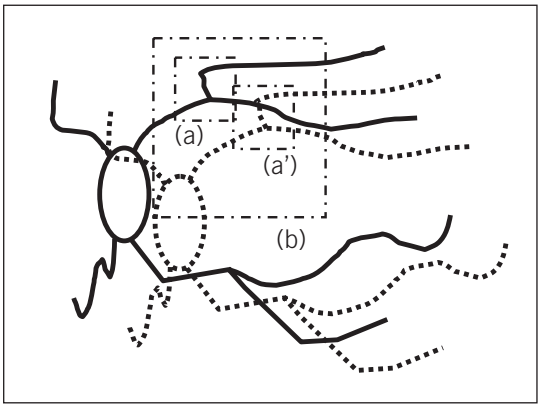

Fig. 6. Manual or automated tracking

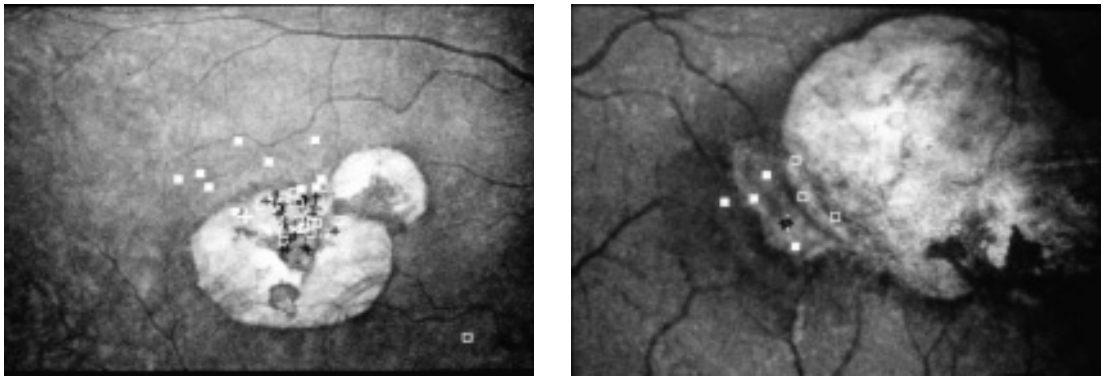

Fig. 7. Left image is right eye, right image is left eye. Black crosses are fixation sample locations. Solid white squares are seen suprathreshold stimuli locations

EXAMPLES AND DISCUSSION

Figure 7 shows on the left side the infra-red SLO fundus image of the right eye of a 45 year old male. A sharply outlined dry atrophic scar due to previous laser treatments for POHS replaces the original central macular area. On the right side of figure 7 is the infra-red SLO fundus image of the left eye of the same person. This eye was also treated before with laser for the same condition, however until recently the foveolar area had been spared. The central bouquet of foveal cone receptors that are responsible for the still 20/20 visual acuity in this eye can be unequivocally located through microperimetric sampling and plotting of the exact position of the projected fixation cross during a manual static microperimetry session. Photopic background conditions have been used for this data collection. It also appears that this retinal locus of fixation is very steady, singular, does not have nystagmoid components and has quite a small bivariate area of deviation. This is valuable clinical information impossible to obtain with other techniques, and it has helped us to decide on a medical treatment rather than passive follow-up, destructive or selective laser therapy. Furthermore, the foveal location has now been undermined by an active extension of the pathology at the nasal edge of the scar. This well-defined zone of subretinal abnormality is itself surrounded by a semicircular area of retinal edema. Infra-red confocal scanning is particularly suited to visualize the presence of even small areas of retinal and sub-retinal edema, without the necessity of more invasive fluorescein injections. This visualization is much more difficult with either conventional color fundus illumination or non-confocal scanning. The

explanation of this is two-fold. First, there is a reduced absorption of infra-red by the conventional pigments in the eye and second, small variations in retinal and sub-retinal IR multiple scattering determine the amount of light returning from the deeper retina through the relaxed virtual confocal aperture. Manual static microperimetry reveals that both areas do not correspond to a threshold scotoma using a slightly supra-threshold intra-retinal reference stimulus intensity value

What findings do microperimetric testing for the right eye reveal to us that are clinically significant? It is remarkable that a set of fixation samples is found within the dense scotoma corresponding to the laser treatment scar and this set is also approximately located at the original foveal area. We usually register unbiased retinal fixation locations by sampling concurrently with another test which has been explained to the subject. Conveniently this test may be a manual static supra-thresholding microperimetry. The subject will then be asked to look in the direction of the fixation cross as good as s/he can, but not worry too much if it disappears from time to time. Such conditions of testing nicely demonstrate the phenomenon of pseudo-central fixation.[65] Even under monocular testing conditions, the fixation reflex which is triggered by the visual and motor cortex, will force the subject to try to see the fixation target with a non-functional foveal area most of the time. This motor reflex reveals the presence of a binocular congruent (0,0) motor reference. In other publications we illustrated cases where the retinal fixation was extra-macular and also congruent in both eyes.[60] The strong persistence of the fixation reflex, even when foveal functioning has been lost in one eye, explains the abnormal low clinical acuity of counting fingers at 3 feet in this eye. In general, binocular correspondence of retinal fixation loci gives rise to transitional patterns of fixation behavior in both eyes over time, even when central fixation is permanently lost in both eyes.[61] We think that the loss of the original (0,0) motor foveal reference and a physiologic imbalance in the strength of the eye muscles may then favor the gradual development of eccentric fixation patterns into the right superior quadrants of the retina.[12] Interestingly, in a number of normal left-handed subjects, we found that a provoked pseudo-fixation tended to drift towards the left superior quadrant when the fixation target was intentionally removed from a manual static microperimetry test. The subjects were not told the real purpose of the test, except for looking as good as possible towards the direction where the fixation cross was last seen.

The documentation of the retinal fixation loci, pseudo-fixation tendencies and potential acuities in various retinal locations has a significant psychological impact on the patient. In this case, the subject was severely depressed, knowing that one eye had a CF acuity, and the other eye might also lose reading vision. Therefore he faced the loss of independent living. In this case, a forced observation of the acuity letter E superiorly to the scar in the right eye resulted in an acuity of 20/60 with the 4AFC test. It is a remarkable observation that subjects regain a lot of confidence when they discover that even a bad eye with a relatively large dense central scotoma can regain useful visual acuity if the retinal locus of fixation moves to a better functional area when binocular interactions will permit this. The important lesson here is to continue aggressively treating an apparent lost eye to keep the lesion as small and dry as possible, definitely so if it would tend to extend into an area of potential good eccentric fixation. The phenomenology of pseudo-central fixation also tells us that an apparent improvement in a treated eye, over time, may not solely be a beneficial result of the actual treatment but rather a consequence of binocular interactions and shifting retinal loci of fixation. Therefore in follow-up studies of a macular treatment, tracking of both acuity and fixation patterns in both eyes over time is important.

Figure 8 illustrates how difficult it is to assess the efficacy of a treatment modality - in this case photodynamic therapy for ARM - without access to detailed microperimetric data over time. The right column of figures corresponds to the left eye, the left column corresponds to the right eye. The upper 4 pictures and lower 4 pictures were taken one year apart. The uneven rows of pictures show representative location samples of a dense scotoma with associated fixation samples using a photopic background. The even rows of pictures show the potential acuity in corresponding fixation locations.

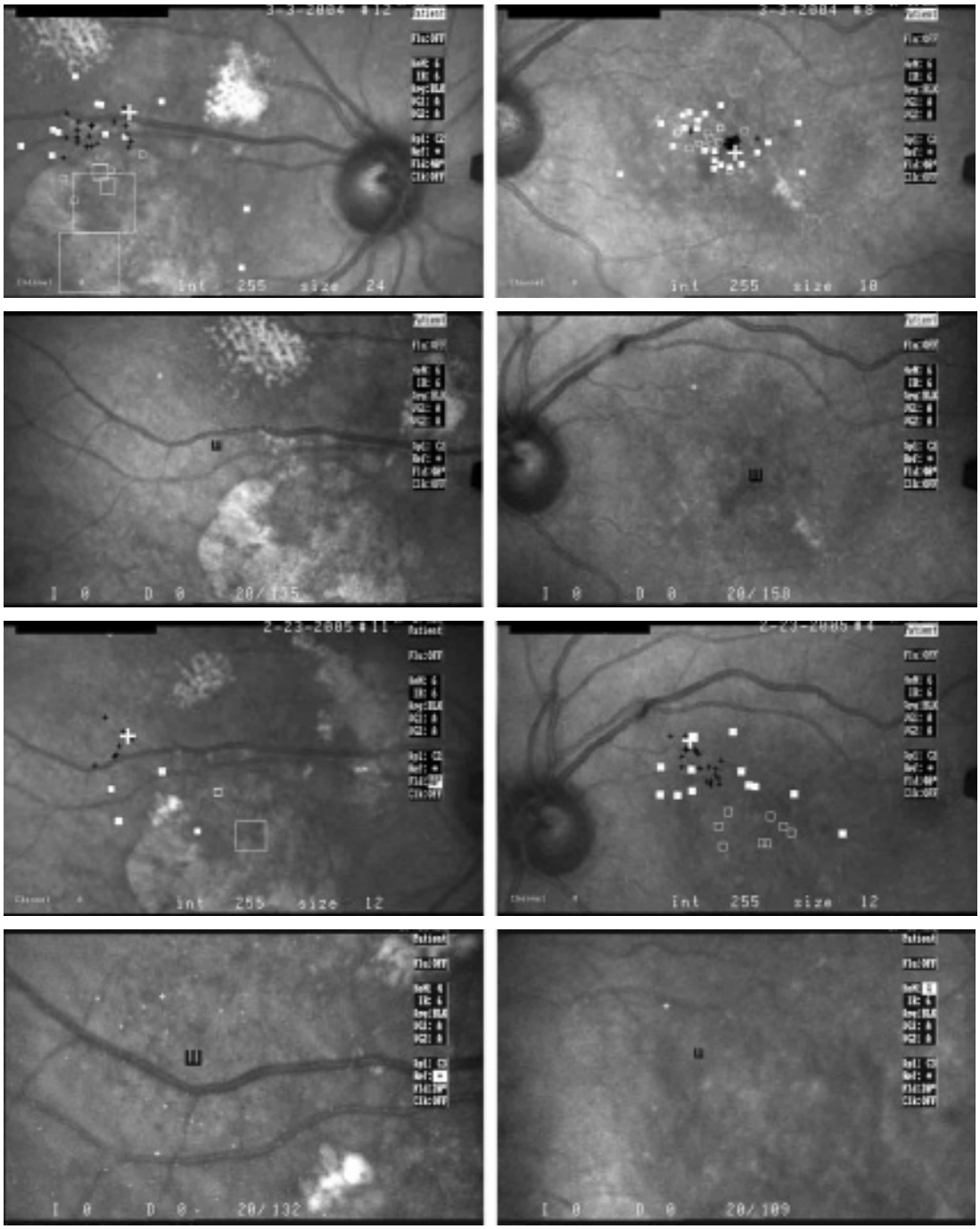

Fig. 8. Right eye on the left side, Left eye on the right side. Upper 4 images from March 2004 exam, lower 4 images from Feb 2005 exam. Odd rows are stimuli locations and fixation samples. Even rows show potential acuity location and measurement

The right eye had an established atrophic scar due to destructive laser treatment before the first examination. Some areas of suspected leakage are present superiorly and merit further ablation to dry the adjacent retina. Eccentric fixation samples are clustered into a fairly defined eccentric locus of fixation in the superior and right quadrant of the retina. The potential 4AFC measured acuities are similar during the two consecutive examinations one year apart, respectively 20/132 and 20/135.
The left eye had had non-destructive PDT treatment elsewhere before our first examination. Under photopic background conditions a partial dense central scotoma was present with preservation of the central foveal fixation pattern that was lost though upon lowering the background. The corresponding acuity was 20/158. One year later, under photopic conditions, the central foveal area was no longer functional, but another binocular conjugate eccentric retinal locus of fixation had further developed with a surprising better acuity of 20/109. It appears from these findings that PDT itself did not preserve foveal functioning and would as such have been responsible for the better acuity over time. It did however most certainly avoid patient's complaint of a possibly abrupt decline in visual functioning had the macular area been ablated by destructive laser action in the first place. The surgeon's decision whether to treat such lesions destructively or selectively will ultimately depend on different factors such as the size, location and aggressiveness of the lesion, the patient's understanding of the psychophysical aspects of the disease over time and whether this is the first or second eye being affected. Formal treatment rules or algorithms seem difficult to establish, especially within the context of promising new non-destructive treatments based on anti-angiogenesis medication.

CONCLUSION

Previous milestones in perimetry have included the invention of the Goldmann perimeter in 1945 [10-11,42] and the automated or computerized perimeter around 1975.[8,25] Both are cupola perimeters employing a Newtonian free field of indirect viewing of a Ganzfeld "white light" illumination. The Goldmann uses typically a kinetic technique in which the observer controls the position of the stimulus. The automated machines project a sequence of static stimuli of which the intensity and position are determined by a computer. Both instruments have some passive fixation control capability, but do not actively correct for fixation shifts. We consider SLO microperimetry a third milestone development that uses a direct laser line raster scanning onto the retina to project either static or kinetic stimuli with two different distinct wavelengths used for the photopic and scotopic system. The Maxwellian view is helpful in controlling retinal illuminance. Microperimetry has an efficient manual or automated implementation for correcting fixation shifts, resulting in scotoma maps of high resolution - and thus justifying its name. Concurrent fixation and acuity mapping is possible as well. All three kinds of perimetry share robustness of calibration and suitability for standardization. Microperimetry can be both an efficient screening and advanced diagnostic application. As the examples have illustrated, these tests render the SLO highly useful in the diagnosis, laser treatment or low vision rehabilitation of maculopathies such as ARM. Non-mydriatic infra-red confocal imaging and graphics animation are two factors that make this instrument also a first choice for pediatric psychophysics. It is helpful in the diagnosis of neuro-ophthalmologic diseases, malingering and open angle glaucoma. It is a highly didactic tool for the education of patients and their family, and compared to other testing procedures it is generally very well tolerated by them. The SLO does have impressive ophthalmoscope and fundus camera like diagnostic capabilities as well: a unique confocal IR imaging and complimentary red-free imaging mode, and high-speed recording of the fluorescein and indocyanin dye transits. Last but not least, in our opinion a combination with high-speed SD-OCT using the high quality video IR image as a fiducial landmark, would turn the SLO into a first line diagnostic combination device conferring onto this instrument a status in ophthalmology that is comparable to the slit lamp and automated refractometer.

REFERENCES

(1) ANDERSON D.R. – Perimetry with and without Automation (2nd edition). CV Mosby, St. Louis MO 1987; Ch 14: 330-344
(2) AVILA M.P., JALKH A.E., MAINSTER M.A., TREMPE C.L., WEITER J.J., SCHEPENS C.L. – Photofield mapping in the evaluation and management of subretinal neovascularization. Ann Ophthalmol 1985; 17: 13-19
(3) AWAYA S., OHASHI T., ASONO T. – Spot scotometry; a new method to examine scotomas under direct ophthalmoscopy by using Visuscope (Euthyscope). Jpn J Ophthalmol 1972; 16: 144-157
(4) BEKESY G.v. – A new audiometer. Acta oto-laryng (Stockholm) 1947; 35: 411-422
(5) BROWN B., ADAMS A.J., COLETTA N.J., HAEGERSTROM-PORTNOY G. – Dark adaptation in age-related maculopathy. Ophthalm Physiol Opt 1986; 6: 81-84
(6) CORNSWEET T.N. – The staircase method in psychophysics. Am J Psychol 1962; 75: 485-491
(7) CREELMAN C.D., MACMILLAN N.A. – Detection Theory: A user's guide. Cambridge university press 1991; Ch 8 (Adaptive methods for estimating empirical thresholds): 183-208
(8) FANKHAUSER F. – The development of computerized perimetry. In: Whalen W.R., Spaeth G.L. (eds.) Computerized Visual fields. Slack, Thorofare NJ 1985; Ch 2: 11-27
(9) FERRIS F., SPERDUTO R. – Standardized illumination for visual acuity testing in clinical research. Am J Ophthalmol 1982; 94: 97-98
(10) GOLDMANN H. – Ein selbregistrierendes Projektionskugelperimeter. Ophthalmologica 1945; 109: 71-79
(11) GOLDMANN H. – Grundlagen exakter Perimetrie. Ophthalmologica 1945; 109: 57-70
(12) GUEZ J.E., LE GARGASSON J.F., RIGAUDIERE F., O'REGAN J.K. – Is there a systematic location for the pseudo-fovea in patients with central scotoma? Vision Res 1993; 33: 1271-1279
(13) HIGGINS G.C., STULTZ K.F. – Frequency and amplitude of ocular tremor J Opt Soc Am 1953; 43: 1136-1140
(14) INATOMI A. – A simple fundus perimetry and fundus camera. Doc Ophthalmol Proc 1978; 19: 359-362
(15) INATOMI A. – Fundus perimetry. Jpn J Clin Ophthalmol 1967; 21: 1109-1110
(16) JALKH A.E., AVILA M.P., TREMPE C.L., SCHEPENS C.L. – Management of choroidal neovascularization within the foveal avascular zone in senile macular degeneration. Am J Ophthalmol 1983; 95: 818-825
(17) JAMARA R.J., VAN DE VELDE F., PELI E. – Scanning eye movements in homonymous hemianopia documented by scanning laser ophthalmoscope retinal perimetry. Optom Vis Sci 2003; 80: 495-504
(18) KANI K., ENO N., ABE K., ONO T. – Perimetry under television ophthalmoscopy. In: Greve E.L. (ed.) Proceedings of the second international visual field symposium, Tübingen 1976. Doc Ophthalmol Proc 1977; 14: 231-236
(19) KANI K., OGITA Y. – Fundus controlled perimetry. Doc Ophthalmol Proc 1978; 19: 341-350
(20) KANI K., OGITA Y. – Fundus controlled perimetry. Folia Ophthalmol Jpn 1979; 30: 141-149
(21) KELLEY J.S. – Use of the argon aiming beam in visual function testing. Ann Ophthalmol 1978; 10: 1687-1689
(22) KOHAYAKAWA Y., KASHIWAGI K., MATSUMURA I. – Ophthalmologic apparatus and method of compounding the image of an eye to be examined. US patent 1991: 5 037 194
(23) LUDVIGH E. – Extrafoveal visual acuity as measured with Snellen test-letters. Am J Ophthalmol 1941; 24: 303-310
(24) LYNN J.R., FELMAN R.L., STARITA R.J. – Principles of perimetry. In: Ritch R., Schields M.B., Krupin T. (eds.) The Glaucomas. CV Mosby, St Louis MO 1996; 491-521
(25) LYNN J.R., TATE G.W. – Computer controlled apparatus for automatic visual field examination. US patent 1975: 3 883 234
(26) MEYERS M.P. – The use of the visuscope for mapping a ''field'' of retinal function. Am J Ophthalmol 1959; 47: 577-681
(27) NACHMIAS J. – Two dimensional motion of the retinal image during monocular fixation. J Opt Soc Am 1959; 49: 901-908
(28) NAS-NRC COMMITTEE ON VISION – Recommended standard procedures for the clinical measurements and specification of visual acuity. Adv Ophthalmol 1980; 41:103-148
(29) NICHOLS P.F. – Evaluation of choroidal neovascular membranes by octopus perimetry. Retina 1988; 8: 24-29

(30) OHTA Y., MIYAMOTO T., HARASAWA K. – Experimental fundus photo perimeter and its application. Doc Ophthalmol Proc 1978; 19: 351-358
(31) PAPRITZ H. – Bowl perimeter. US patent 1948: 2 441 031
(32) PELI E., AUGLIERE R.A., TIMBERLAKE G.T. – Feature-based registration of retinal images. IEEE trans on med imaging 1987; MI-6: 272-278
(33) POMERANTZEFF O., LEE P.F., HAMADA S., DONOVAN R.H., MUKAI N., SCHEPENS C.L. – Clinical importance of wavelengths in photocoagulation. Trans Acad Am Ophthalmol Otolaryngol 1971; 75: 557-568
(34) POMERANTZEFF O., SCHEPENS C.L. – Studies in photocoagulation. Br J Ophthalmol 1964; 48: 306-310
(35) PRATT W.K. – Digital Image Processing. Wiley, New York NY 1991; Ch 20 (Image detection and registration): 651-673
(36) PRITCHARD R.M. – Stabilized images on the retina. Sci Am 1961; 204(6): 72-78
(37) RATLIFF F., RIGGS L.A. – Involuntary motions of the eye during monocular fixation. J Exp Psychol 1950; 40: 687-701
(38) RIGGS L.A., ARMINGTON J.C., RATLIFF F. – Motions of the retinal image during fixation. J Opt Soc Am 1954; 44: 315-321
(39) ROSE R.M., TELLER D.Y., RENDLEMAN P. – Statistical properties on staircase estimates. Perception & Psychophysics 1970; 8: 199-204
(40) SALEH B., TEICH M.C. – Fundamentals of Photonics. Wiley, New York NY 1991; Ch 3 (Beam optics): 80-107
(41) SALEH B., TEICH M.C. – Fundamentals of Photonics. Wiley, New York NY 1991; Ch 20 (Acousto-optics): 799-830
(42) SCHEPENS C.L. – Le périmètre à coupole de Goldmann. Bull Soc Belge Ophtalmol 1945; 83: 17-22
(43) SCHEPENS C.L. A propos de la périmétrie. Enseignements receuillis dans quelques cliniques londoniennes. Bull Soc Belge Ophtalmol 1939; 78: 73-85
(44) SCHOESSLER J.P., UNIACKE C.A. – Perimetry: a need for standardization. Am J Optom Physiol Opt 1977; 54: 699-702
(45) SCHOESSLER J.P., UNIACKE C.A. – Standardization of the Bausch and Lomb Autoplot Tangent Screen. Am J Optom Physiol Opt 1977; 54: 782-786
(46) SOLON L.R., ARONSON R., GOULD G. – Physiological implications of laser beams. Science 1961; 134: 1506-1508
(47) STEINMAN R.M., HADDAD G.M., SKAVENSKI A.A., WYMAN D. – Miniature eye movements. Science 1973; 181: 810-819
(48) STILES W.S. – The directional sensitivity of the retina and the spectral sensitivities of the rods and cones. Proc Roy Soc (London) 1939; B127: 64-105
(49) STILES W.S., CRAWFORD B.H. – The luminous efficiency of rays entering the eye pupil at different points. Proc Roy Soc (London) 1933; B112: 428-450
(50) SUNNESS J.S., JOHNSON M.A., MASSOF R.W., KAYS D.L. – Wilmer fundus camera stimulator. Applied Optics 1987; 26: 1487-1491
(51) SUNNESS J.S., JOHNSON M.A., MASSOF R.W., MARCUS S. – Retinal sensitivity over drusen and nondrusen areas: A study using fundus perimetry. Arch Ophthalmol 1988; 106: 1081-1084
(52) SUNNESS J.S., SCHUCHARD R.A., SHEN N., RUBIN G.S., DAGNELIE G., HASELWOOD D.M. – Landmark driven fundus perimetry using the scanning laser ophthalmoscope. Inv Ophthalmol Vis Sci 1995; 36: 1863-1873
(53) TANASSI C., PIERMAROCCHI S., BUSCEMI P.M. – Instrument for eye examination and method. US patent 2004: 6 705 726
(54) TAYLOR M.M., CREELMAN C.D. – Pest: efficient estimates on probability functions. J Acoust Soc Am 1967; 41: 782-787
(55) TIMBERLAKE G.T., MAINSTER M.A., SCHEPENS C.L. – Automated clinical visual acuity testing. Am J Ophthalmol 1980; 90: 369-373
(56) TIMBERLAKE G.T., MAINSTER M.A., WEBB R.H., HUGHES G.W., TREMPE C.L. – Retinal localization of scotomata by scanning laser ophthalmoscopy. Inv Ophtalmol Vis Sci 1982; 22: 91-97
(57) TIMBERLAKE G.T., VAN DE VELDE F.J., JALKH A.E. – Clinical use of scanning laser ophthalmoscope retinal function maps in macular disease. Lasers and light in ophthalmol 1989; 2: 211-222
(58) TRANTAS N.G. – Applications et resultats d'un moyen simple d'examen de la photosensibilité de la rétine. Bull Soc Ophtalmol Fr 1955; 55: 499-513

(59) TREMPE C.L., MAINSTER M.A., POMERANTZEFF O., AVILA M.P., JALKH A.E., WEITER J.J., MCMEEL J.W., SCHEPENS C.L. – Macular photocoagulation. Optimal wavelength selection. Ophthalmology 1982; 89: 721-728
(60) VAN DE VELDE F. – Micropérimétrie et dégénérescence maculaire liée à l'age. Safran A.B., Assimacopoulos A. (eds.) In: Le handicap visuel: déficits ignorés et troubles associés. Masson, Paris 1997; 205-212
(61) VAN DE VELDE F.J. – Quantitative SLO microperimetry for clinical research in age related maculopathy. In: Dean Yager (ed.) Noninvasive assessment of the visual system (OSA TOPS). Opt Soc of America, Washington D.C. 1997; 11: 42-47
(62) VAN DE VELDE F.J. – Scannning laser ophthalmoscopy optimized testing strategies for psychophysics. In: Fercher A.F. (ed.) Lasers in Ophthalmology IV. Proc SPIE, Bellingham WA 1996; 2930: 79-90
(63) VAN DE VELDE F.J., JALKH A.E., ELSNER A.E. – Microperimetry with the scanning laser ophthalmoscope. In: MILLS R.P., HEIJL A. (eds.) Perimetry Update 1990/91. Kugler publications, New York NY 1991; Ch 2: 93-101
(64) VAN DE VELDE F.J., TIMBERLAKE G.T., JALKH A.E., SCHEPENS C.L. – La micropérimétrie statique avec l'ophtalmoscope à balayage laser with the laser scanning ophthalmoscope. Ophtalmologie 1990; 4: 291-294
(65) VON NOORDEN G.K., MACKENSEN G. – Phenomenology of eccentric fixation. Am J Ophthalmol 1962; 53: 642-659
(66) WALD G. – Human vision and the spectrum. Science 1945; 101: 653-658
(67) WALD G. – The spectral sensitivity of the human eye. J Opt Soc Am 1945; 35: 187
(68) WALRAVEN J., ENROTH-CUGELL C., HOOD D.C., MACLEOD D., SCHNAPF J.L. – The control of visual sensitivity. In: Spillmann L., Werner J.S. (eds.) Visual perception: the neurophysiologic foundations. Academic Press, San Diego CA 1990; Ch 5: 53-101
(69) WEBB R.H., HUGHES G.W. – Scanning laser ophthalmoscope. IEEE Trans Biomed Eng 1981; BME-28: 488-492
(70) WESTHEIMER G. – The Maxwellian view. Vis Res 1966; 6: 669-682
(71) WYSZECKI G., STILES W.S. – Color Science: concepts and methods, quantitative data and formulae (2nd edition). Wiley, New York NY 1982; Ch 2 (the eye): 83-116
(72) WYSZECKI G., STILES W.S. – Color Science: concepts and methods, quantitative data and formulae (2nd edition). Wiley, New York NY 1982; Ch 4 (photometry): 249-277
(73) WYSZECKI G., STILES W.S. – Color Science: concepts and methods, quantitative data and formulae (2nd edition). Wiley, New York NY 1982; Ch 5 (visual equivalence matching): 278-485
(74) WYSZECKI G., STILES W.S. – Color Science: concepts and methods, quantitative data and formulae (2nd edition). Wiley, New York NY 1982; Ch 7 (visual thresholds): 514-581
(75) ZARET M.M., BREININ G.M., SCHMIDT H., , RIPPS H., SIEGEL I.M., SOLON L.R. – Ocular lesions produced by an optical maser (laser). Science 1961; 134: 1525-1526
(76) ZARET M.M., RIPPS H., SIEGEL I.M., BREININ G.M. – Laser photocoagulation of the eye. Arch Ophthalmol 1963; 69: 97-104

.....

Corresponding address:

Frans J. Van de Velde MD
2 Hawthorne Place, 15-O
Boston MA 02114
vdv@sloresearch.org